Clays and Clay Minerals, Vol. 50, No. 1, 82–98, 2002.

TOBELITIZATION OF SMECTITE DURING OIL GENERATION IN OIL-SOURCE SHALES. APPLICATION TO NORTH SEA ILLITE-TOBELITE-SMECTITE-VERMICULITE

VICTOR A. DRITS[1], HOLGER LINDGREEN[2,*], BORIS A. SAKHAROV[1], HANS JØRGEN JAKOBSEN[3], ALFRED L. SALYN[1] AND LIDIA G. DAINYAK[1]

[1] Institute of Geology, Russian Academy of Science, Pyzhevsky per D.7, 109017 Moscow, Russia
[2] Clay Mineralogical Laboratory, Geological Survey of Denmark and Greenland, Thoravej 8, DK2400 Copenhagen NV, Denmark
[3] Instrument Centre for Solid-State NMR Spectroscopy, Department of Chemistry, University of Aarhus, DK8000 Aarhus C, Denmark

Abstract—Illite-smectite (I-S) minerals isolated from Upper Jurassic oil-source rock shales from Denmark and the North Sea have been investigated by X-ray diffraction, thermal analysis, infrared, Mössbauer, and solid-state nuclear magnetic resonance spectroscopies and chemical analysis. Detailed structures have been determined in order to reveal the diagenetic transformation mechanism in these shales. Generally, in oil-source rocks of sedimentary basins, oil generation takes place simultaneously with the diagenetic transformation of I-S. We demonstrate a link between the two reactions: NH_3 released from kerogen during maximum oil generation is fixed as NH_4^+ in the NH_4-bearing mica or tobelite layers formed from smectite or vermiculite layers in I-S, in a diagenetic interval which we name the 'tobelitization window'. Due to this solid-state transformation, mixed-layer structures have been formed consisting of interstratified illite, tobelite, smectite and vermiculite layers (I-T-S-V) and having maximum ordering of illite + tobelite and smectite layers for R = 1. The tobelitization of smectite in I-S is probably typical for all oil-source rock shales.

Key Words—Ammonium, Diagenesis, Illite-smectite, Jurassic, North Sea, Oil-Source Rock, Shales.

INTRODUCTION

Mixed-layer illite-smectite (I-S) is a typical component of shales. The structure consists of illite and smectite interlayers interstratified in variable proportions and distribution patterns. Both the amount of illite layers and tendency to ordered distribution of illite and smectite layers within individual MacEwan microcrystals increase during diagenesis in shales (Shutov *et al.*, 1969a,b; Perry and Hower, 1970; Hower *et al.*, 1976; Lindgreen and Hansen, 1991). Several structural mechanisms have been proposed to describe this illitization process (*e.g.* Altaner and Ylagan, 1997): (1) a solid-state transformation characterized by tetrahedral Al for Si substitution and subsequent dehydration and fixation of cations in interlayers of smectite or of smectite in I-S crystallites (Shutov *et al.*, 1969a,b; Pollard, 1971; Hower *et al.*, 1976; Drits *et al.*, 1997a); (2) a solid-state layer-by-layer neoformation in smectite or I-S crystallites (Bell, 1986; Bethke and Altaner, 1986; Drits *et al.*, 1996); or (3) in sandstones and bentonites, a smectite dissolution and illite neoformation through precipitation (Nadeau *et al.*, 1985; Nadeau and Bain, 1986) or growth according to the law of proportional effect (Środoń *et al.*, 2000).

* E-mail address of corresponding author: hl@geus.dk

It is generally assumed that temperature is the main control in this reaction and the formation of illite layers takes place by fixation of K. In oil-source rocks of sedimentary basins, oil generation takes place simultaneously with the diagenetic transformation of I-S (Hunt, 1979; Heling and Teichmüller, 1974; Foscolos and Powell, 1979; Dypvik, 1983; Durand, 1985; Hansen and Lindgreen, 1989). This coincidence may be due to the fact that the two totally different reactions have the same temperature of activation, but a more direct link may be interaction of I-S with decomposed organic matter. Stevenson (1960) suggested that NH_3 released from the decomposition of organic matter can be fixed in illite interlayers as NH_4. Cooper and Abedin (1981) found that the amount of fixed NH_4 in Tertiary Gulf Coast shales increased with depth and eventually constituted 7% of the fixed interlayer cations in clay fractions. Williams *et al.* (1989, 1992) investigated NH_4-bearing sandstones and mudstones from Gulf Coast Tertiary sediments and found that NH_4, released during oil generation from organic matter, migrated with oil through sandstones to become incorporated into clay-mineral structures. Hansen and Lindgreen (1989) and Lindgreen and Hansen (1991) using simulated X-ray diffraction (XRD) patterns and high-resolution electron microscopy (HREM) studied I-S formed during diagenesis in Upper Jurassic oil-source shale of the North Sea area. They concluded that detrital I-S with a tendency of the layer types to segregation are diagenetically trans-

formed to I-S having the maximum degree of ordering possible (R = 1). Lindgreen (1994) found for the same rocks that with increasing depth of sample, the ratio NH_4/K for soluble cations in the porefluids of core samples increased as did the same ratio for fixed cations in interlayers of the I-S structures and concluded that NH_4 fixation may be a general process during burial diagenesis in oil-source rocks.

Structural study of I-S in shales and especially in oil-source shales is difficult because clay fractions extracted from shale samples are typically a mixture of detrital and authigenic minerals and, moreover, the complex structure of I-S in shales cannot be determined by conventional XRD techniques. A new methodological complex consisting of three methods has been developed and tested on several representative samples of the Upper Jurassic and Cambrian alum black oil-source shales (Drits *et al*., 1997a; Sakharov *et al*., 1999; Lindgreen *et al*., 2000). The first, the multi-specimen method, determines the detailed structural and probability parameters of the interstratification in multi-component mixed-layer minerals (Drits *et al*., 1997b; Sakharov *et al*., 1999). In contrast to most published simulations of XRD patterns for I-S models, in this method, agreement between calculated and experimental XRD patterns is obtained not only for positions, but also for intensity and profiles of the reflections. Furthermore, such agreement was obtained between one structural model and the XRD patterns of different specimens prepared from each sample subjected to different treatments (saturation by different interlayer cations, glycolation, *etc*.). This method revealed the sequential structure transformation of illite-smectite-vermiculite during diagenesis of the North Sea Upper Jurassic oil-source shales to be a solid-state transformation of smectite interlayers into mica (Drits *et al*., 1997b). The results of this work confirmed the conclusions of Lindgreen (1991). The second method determined: (1) the average content of NH_4; and (2) the distribution patterns of interlayer K and NH_4 in NH_4-bearing I-S structure (Drits *et al*., 1997a). Application of this method showed that NH_4-bearing I-S from the North Sea and Cambrian Alum shales from the Baltic area consist of irregularly interstratified K-bearing 9.98 Å illite, NH_4-bearing 10.33 Å tobelite and expandable layers (Drits *et al*., 1997a; Lindgreen *et al*., 2000). The third method provides semiquantitative determination of *trans*-vacant (*tv*) and *cis*-vacant (*cv*) 2:1 layers in I-S by thermal analysis (Drits *et al*., 1998b). It is based on the fact that smectites and illites consisting of *cv* 2:1 layers have dehydroxylation temperatures 100° to 200°C higher than those consisting of *tv* 2:1 layers (Drits *et al*., 1995). In contrast to XRD methods, this technique can be applied to I-S having a turbostratic structure, such I-S being widespread in shales.

In this work simulation of the experimental XRD patterns, thermal analysis and IR spectroscopy have been applied for a large number of samples from the North Sea Upper Jurassic shales which is the most important oil-source rock in the North Sea (Thomsen *et al*., 1983). For comparison, samples from the immature Upper Jurassic shales in the Danish Subbasin of the Norwegian–Danish Basin are included. Comparison of the results obtained by these methods with those obtained previously by Lindgreen (1994), Drits *et al*. (1997a,b) and Lindgreen *et al*. (2000) has provided a new insight into specific features of the structural mechanism of I-S transformation during oil generation as well as into the origin and parent source of detrital material.

SAMPLE MATERIALS

Cuttings (hand-picked) and core samples of shales of Upper Jurassic (Kimmeridgian-Volgian-Ryazanian) age from the Mandal, Farsund and Haugesund Formations in the Central Trough, North Sea, and from the Børglum, Sauda and Tau Formations in the Norwegian–Danish Basin (including the Danish Subbasin) have been studied. The cuttings include the Danish wells M8, U1 and I1 and the Norwegian wells 2/7-3 and 2/11-1; core samples came from wells E1, and 2/11-1 as well as from Danish wells East Rosa 3/3A, SE Igor 1, N. Jens 1, Jens 1, Iris 1, Jeppe 1 and Elin 1. Studied samples from the Danish Subbasin include core samples from Frederikshavn 1, Uglev 1, Børglum 1 and Haldager 1 (Figure 1). The samples investigated represent the interval from onset to maximum oil generation. Details of the samples and their location were previously given by Hansen and Lindgreen (1989) and Lindgreen and Hansen (1991).

METHODS

Chemical pretreatment

The samples were pretreated by removal of organic matter and Fe and Al oxides, and the mixed-layer fraction was isolated by centrifugation (Hansen and Lindgreen, 1989) yielding particles predominantly <500 Å in diameter and <100 Å thick (Lindgreen *et al*., 1992). By this method, detrital illite was removed. The mixed-layer fractions were saturated with K^+ and Mg^{2+} by repeated washings using chloride solutions, excess chloride being removed by washing with water. Oriented specimens were prepared by the pipette method using 2.5 mg/cm^2 of specimen and analyzed air-dried and after glycolation for three days at 60°C in glycol vapor. Potassium-saturated samples were heated at 150°C to contract the expandable layer thickness to 9.98 Å and the patterns were recorded immediately afterwards, heating being repeated for 5 min before the scan of each peak.

X-ray diffraction

The XRD patterns were obtained using the Philips PW3040 and PW1050 (samples investigated in

https://doi.org/10.1346/000986002761002702 Published online by Cambridge University Press

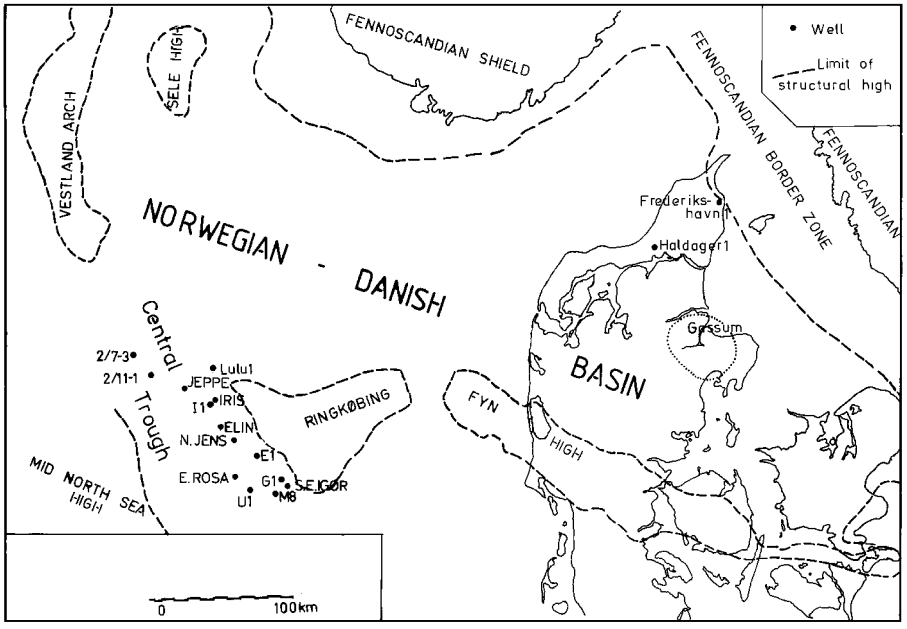

Figure 1. Locations of wells investigated in the Central Trough and the Norwegian–Danish Basin.

Denmark) and the DRON-4 (samples investigated in Russia) diffractometers, employing CoKα and CuKα radiation. The PW 3040 instrument has a curved graphite monochromator and a fine-focus tube. For complete XRD patterns of oriented specimens in the interval 1.5–65°2θ, ¼° fixed divergence and anti-scatter slits were used and intensities were measured for 10 s per 0.1°2θ step. The DRON-4 instrument has a horizontal goniometer supplied with a graphite monochromator which has a set of fine anti-scatter slits (0.1–0.25 mm) together with Soller slits which have an angular aperture of 1.5°. Intensities were measured for 100 s per 0.05°2θ step. Fitting of the XRD patterns within the 2.5–55°2θ region was carried out according to the procedure described by Drits *et al.* (1997b) and Sakharov *et al.* (1999). In the following, I, T, S and V denote illite, tobelite, smectite and vermiculite-like interlayers or layers, respectively, and I-S-V and I-T-S-V denote mixed-layer illite-smectite-vermiculite and illite-tobelite-smectite-vermiculite, respectively. We define expandable layers as smectite and vermiculite if in the glycolated state their interlayers contain two or one layers of glycol molecules, respectively, independent of the nature of the exchangeable cations. Layers with swelling properties which depend on the exchangeable cations are referred to as 'low-charge vermiculite or high-charge smectite' layers (V′-layers). For I-S-V the K content in the illite-like interlayers was 0.75–0.5 atoms per $O_{10}(OH)_2$ for different samples and decreases with the degree of diagenetic transformation of the samples. For I-T-S-V the K and NH_4 contents in illite and tobelite interlayers were 0.75 and 1.0 cations per $O_{10}(OH)_2$, respectively (Drits *et al.*, 1997a,b; Sakharov *et al.*, 1999; Lindgreen *et al.*, 2000). The K, NH_4 and Na cations were placed in the center of mica interlayers. The thicknesses of the illite and tobelite layers in I-T-S-V were found to be 9.98 and 10.33–10.35 Å, respectively (Drits *et al.*, 1997a) whereas for I-S-V the thickness of illite-like layers was variable. The thicknesses of coherent scattering domains (CSDs) were distributed log-normally. The parameters of this distribution were determined using a mean thickness of CSDs and the regression given by Drits *et al.* (1997c) having mean and maximum thicknesses of CSDs as variable parameters.

Thermal analysis

A Stanton Redcroft DTA 673-674 with gas outlet to non-dispersive infrared (IR) H_2O and CO_2 detectors was used to determine quantitatively the amount of structural water released during heating (evolved water analysis, EWA), (Morgan, 1977). The main advantage of this technique is that the loss of hydroxyls is recorded separately and that the amount of structural water released during dehydroxylation can be determined quantitatively and with high sensitivity.

Sodium-saturated samples were heated at 5°C/min in a gas flow of 300 ml N_2 per min. In order to separate dehydration and dehydroxylation processes, the samples were heated first to 200°C and the temperature was then kept constant until the water release had stopped. The samples were then heated in steps to 1000°C at 5°C/min for each step, constant temperature being kept at dehydroxylation peaks.

https://doi.org/10.1346/000986002761002702 Published online by Cambridge University Press

Infrared spectroscopy

Samples were K saturated and heated for 1 h at 150°C before making pellets. The IR spectra were recorded on a Perkin Elmer FTIR spectrometer 1760 from 300 mg KBr pellets with 3 mg of sample. Transmission intensities I_T were recorded at 1 cm^{-1} intervals and for each frequency were transformed to optical density, ln (I_o/I_T), where I_o is the intensity of the incident beam.

The bands were assumed to have Gaussian form, and band position, width at half height and intensity were used in the decomposition procedure as the variable parameters describing individual bands. The quality of the decomposition was estimated from the χ^2 values.

Total chemical analysis

Total chemical analyses were obtained using HF-H_3BO_3 dissolution in teflon bombs (Bernas, 1968), followed by atomic absorption spectrophotometric determination of dissolved K, Na, Mg, Ca, Fe, Al and Si. Each sample was analyzed in a Mg^{2+}-saturated condition.

Mössbauer spectroscopy

Mössbauer spectra were obtained using a constant acceleration spectrometer and a source of ^{57}Co in Pd. Isomer shifts are given relative to the centroid of the spectrum of α-Fe at room temperature. Analyses were performed on selected Na^+-saturated I-S samples at room and liquid nitrogen temperatures and with the absorber plane at an angle of 54.7° to the radiation. Lorentzian line shape was assumed, and all components were assumed to have symmetrical intensity and line-width. Each spectrum was first decomposed into two Fe^{3+} and one Fe^{2+} doublets and then, if necessary, the number of doublets was increased until an acceptable χ^2 value was obtained (Dainyak and Drits, 1987).

Nuclear magnetic resonance spectroscopy

The ^{27}Al and ^{29}Si magic-angle spinning nuclear magnetic resonance (MAS NMR) spectra were recorded on a Varian XL-300 NMR spectrometer (7.1 T) at 78.16 and 59.59 MHz, respectively. For a few samples, spectra were also recorded on Varian VXR-400S (9.4 T) and VXR-500 (11.7 T) spectrometers for comparison of the quadrupolar coupling parameters and chemical shift data determined at the lower (7.1 T) magnetic field strength. All spectra employed home-made high-speed spinning MAS probes of double air-bearing design (Jakobsen *et al.*, 1988) for 7 mm o.d. cylindrical rotors (130 µl sample volume) with a maximum spinning speed of 10 and 16 kHz, respectively. Zirconia (PSZ-700 HP) 7 mm rotors and a spinning speed of 7.2 kHz were used for ^{29}Si observation and Si_3N_4 7 mm rotors with a speed of 9–10 kHz for the ^{27}Al MAS experiments. For selected samples, ^{27}Al MAS spectra were recorded using a spinning speed of 13.5 kHz in 5 mm Si_3N_4 rotors. To ensure quantitative correct determination of the Al^{IV}/Al^{VI} ratios, short radio frequency pulses of 1.5 µs (~π/4 solid pulse) were employed for ^{27}Al. For the ^{29}Si MAS spectra, 3.0 µs pulses and a relaxation delay of 8.0 s were used.

Determination of the structural formulae for I-S

For a mixture of kaolinite and I-S having structural formulae $Si_4Al_4O_{10}(OH)_8$ and

$$R^+_{(x+z)}(Si_{(4-x)}Al_x)[Al_{(2-y-z)}Fe^{3+}_y(Fe^{2+},Mg)_z]O_{10}(OH)_2 \quad (1),$$

respectively, the problem is to determine the values of x, y and z using the chemical composition of the sample and Si/^{IV}Al and ^{IV}Al/^{VI}Al values obtained by ^{27}Al and ^{29}Si MAS NMR spectroscopy.

If the ratio of kaolinite and I-S per $O_{10}(OH)_8$ and $O_{10}(OH)_2$, respectively, is $(1-p)/p$ then the average composition of the sample can be written as:

$$R_{p(x+z)}(Si_{(4-px)}Al_{px})[Al_{(4-2p-py-pz)}Fe^{3+}_{py}(Fe^{2+},Mg)_{pz}]_{(4-2p)}O_{10}(OH)_{(8-6p)} \quad (2)$$

Using the experimental value of a = Si/^{IV}Al, the content of Si and ^{IV}Al per $O_{10}(OH)_{(8-6p)}$ can be determined because

$$Si + {}^{IV}Al = 4;\ (4-px) = 4a/(1+a) \text{ and } px = 4/(1+a) \quad (3)$$

The ratio of the molecular content of SiO_2 determined from the chemical composition and the number of Si atoms per $O_{10}(OH)_{(8-6p)}$ calculated from equation 3 is a multiplier, k, that can be used to determine amount of Al_{tot}, Fe^{2+}, Fe^{3+} and Mg in the structural formula 2. Because the octahedral Al content is equal to the difference between Al_{tot} and Al^{IV}, one can calculate the ^{IV}Al/^{VI}Al values which, within error, should coincide with those determined by NMR. If so, the kaolinite $(1-p)$ content can be calculated from $p = (4-t)/2$ where t is the sum of the octahedral cations in the averaged formula 2. When p is known, formula 2 can easily be transformed into structural formula 1 of I-S.

Determination of the mean number of layers in coherent scattering domains and illite fundamental particles

Drits *et al.* (1998a) proposed a modified version of the Bertaut-Warren-Averbach (BWA) technique to determine the mean number of layers in coherent scattering domains (CSDs) for illite and I-S. Illite-smectites have an irregular structure in the **c*** direction and their basal reflection cannot be analyzed by BWA methods. However, a periodic structure along the **c*** axis may be obtained by K saturation and heating at 150°C prior to XRD. The original computer program to analyze profiles of 00l reflections of the samples based on the mathematical formalism of Drits *et al.* (1998a) was used. In case of I-T-S or I-T-S-V, the saturation by K and dehydration are accompanied by transformation to a structure in which 9.98 Å and 10.33 Å layers are interstratified. When the amount of tobelite is <20%,

https://doi.org/10.1346/000986002761002702 Published online by Cambridge University Press

the difference in the layer thickness can be ignored if only the 001 reflection is used. The validity of this conclusion follows from the calculation of Drits *et al.* (1997) made for interstratified I-T. Środoń *et al.* (1992) showed that the mean number of layers in CSDs, N, and the number of expandable interlayers, w_{S+V}, is related to the mean number of 2:1 layers in illite fundamental particles, $\bar{n}$, *i.e.* the number of 2:1 layers whose interlayers contain fixed K and NH_4, by the equation

$$\bar{n} = N/[(N - 1)w_{S+V} + 1] \quad (4)$$

Atomic force microscopy

Atomic force microscopy (AFM) was carried out on a Rasterscope 4000 instrument using the non-contact mode. The samples were dispersed by ultrasonic treatment in distilled water and a drop was left to dry on a block of highly-oriented pyrolytic graphite. The specimens were scanned at room conditions at a speed of 500 nm/s.

RESULTS

Simulation of the experimental XRD patterns

The XRD patterns of the samples can be divided into three groups. Glycolated group 1 samples have XRD patterns with rather intense 17 Å reflections whose resolution from the low-angle side varies for different samples. This group includes shale samples from the Danish Subbasin and from shallow depth in the Central Trough of the North Sea. Group 2 samples have two distinct reflections in the low-angle diffraction region with 12.8–13.2 Å and 9.8–10 Å spacings, respectively and include most samples from the Central Trough shales taken from depths of >3000–3500 m. Group 3 samples have XRD patterns with a rather sharp and intense 10 Å reflection and a broad low-angle shoulder and include some of the samples from depths >3500 m. For each group, one sample was studied in detail by simulation of the experimental XRD patterns obtained for several specimens of the same sample subjected to different treatments (Drits *et al.*, 1997b). Each sample is a mixture of two mixed-layer phases. The predominant phase (>90%) has alternating illite, smectite and vermiculite interlayers (I-S-V) separated by Al-rich 2:1 layers. The second phase is a kaolinite-illite-vermiculite (K-I-V) containing 90% kaolinite layers. In this work, simulation of the experimental XRD patterns of the samples was carried out using structural and statistical parameters as initial data determined for representative members. The main aim was to determine the most reliable content of the layer types in the I-S-V in the sample collection. Figures 2–5 show simulated and experimental XRD patterns and structural and probability parameters providing the best agreement between the XRD patterns compared.

In the Mg-saturated and glycolated I-S-V phase of group 1 (samples x3, 80, 82, 83, 92, 95, 99, 112), proportions of I, S and V interlayers vary from 65–73, 20–25 and 0.05–0.07, respectively (Figure 2, Table 1). As follows from the conjunction probability parameters p_{ij} (i, j = I, S, V) (Figure 2) the layer-type interstratification has a significant tendency to segregation since $P_{ii} > w_i$ (i = I, S, V). The Mg-saturated and glycolated I-S-V of group 2 (samples x1, x5, x6, x7, x12, x13, x17, 79, 87) contain 0.78–0.86 of illite, 0.10–0.14 of smectite and 0.04–0.08 of vermiculite interlayers (Figure 3, Table 1). The illite and smectite layers in this phase are distributed with the maximum degree of ordering for R = 1 because $P_{SS} = P_{SV} = 0$. However, vermiculite layers preserve their tendency to be segre-

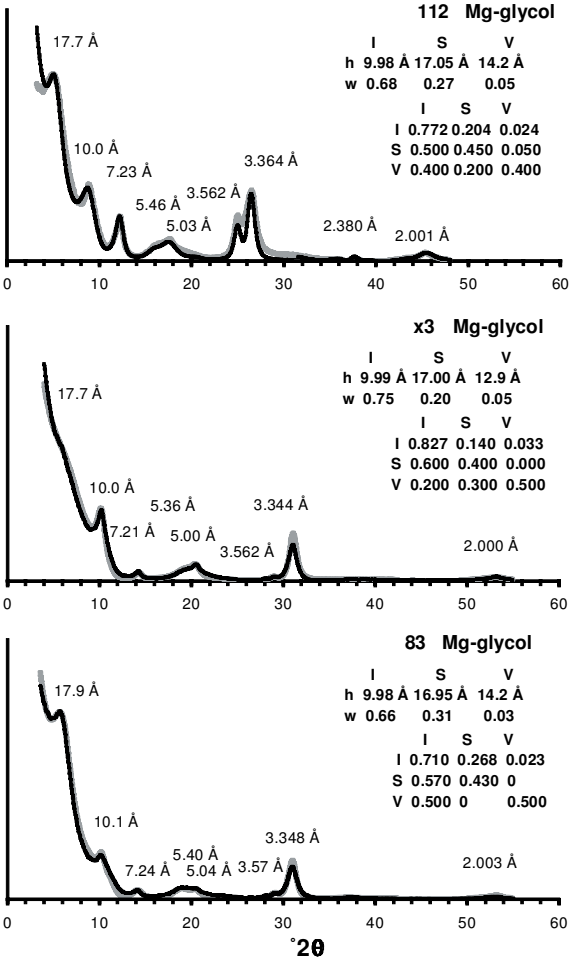

Figure 2. X-ray diffraction patterns of specimens of samples 112, x3 and 83 of group 1 fitted with three components (I, S, V). For each specimen, experimental (thin line, with d-values) and simulated patterns (shaded line) are shown, together with thicknesses (h) and contents (w_i) of the layer types (I: illite; S: smectite; and V: vermiculite layers) and the matrix for the junction probability, $p_{i,j}$, for layer j to follow layer i (i, j = I,S,V). The reflections with spacings of 7.2 Å and 3.56 Å correspond to a kaolinitic phase. Sample 83 contains a small amount (11%) of a high-illitic I-S-V. Co$K\alpha$ radiation.

https://doi.org/10.1346/000986002761002702 Published online by Cambridge University Press

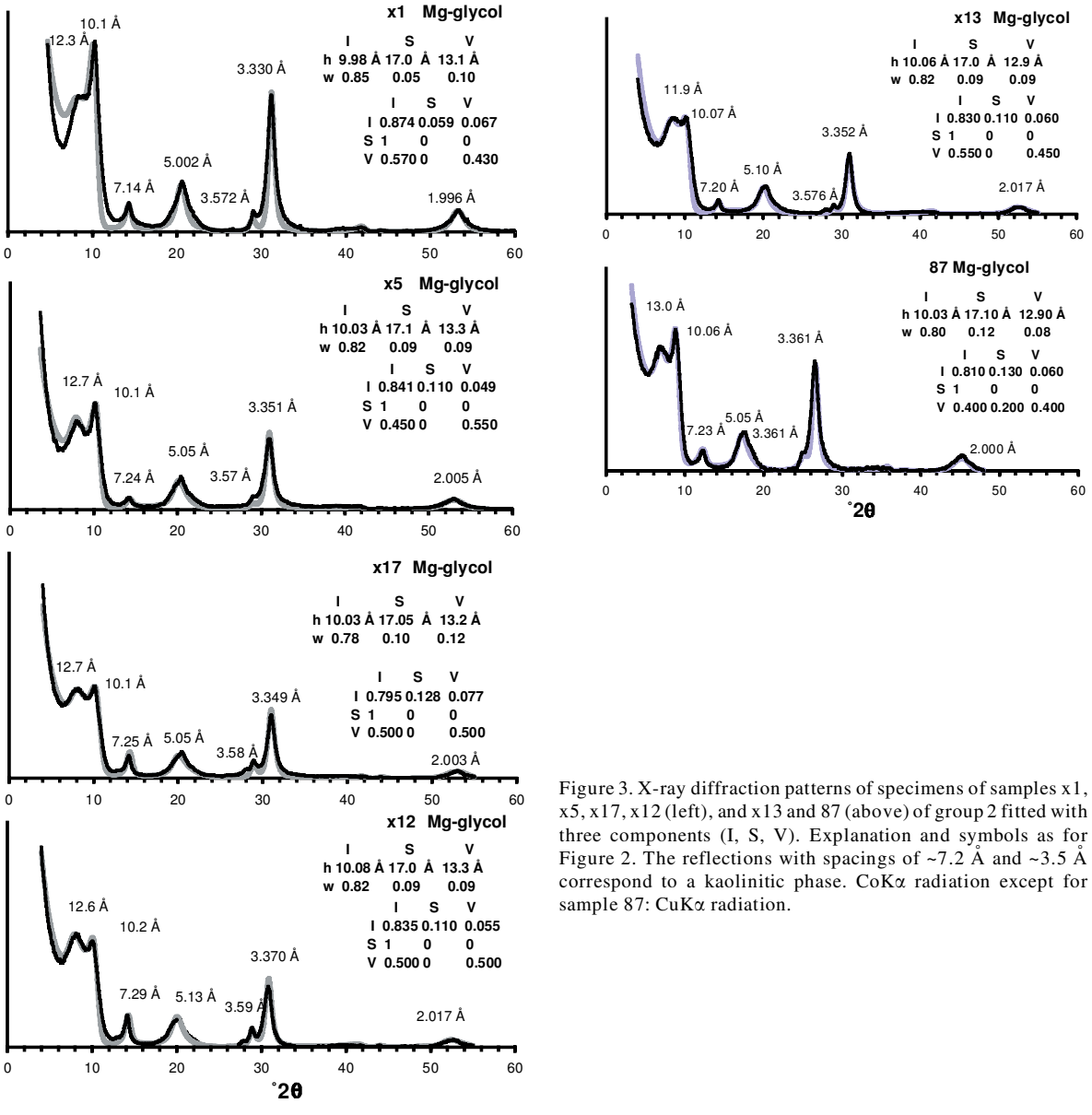

Figure 3. X-ray diffraction patterns of specimens of samples x1, x5, x17, x12 (left), and x13 and 87 (above) of group 2 fitted with three components (I, S, V). Explanation and symbols as for Figure 2. The reflections with spacings of ~7.2 Å and ~3.5 Å correspond to a kaolinitic phase. CoKα radiation except for sample 87: CuKα radiation.

gated ($W_V < P_{VV}$). It is remarkable that the thickness of illite layers for the I-S-V increases up to 10.03 Å (Figure 3) in comparison with 9.98 Å typical for illites (Moore and Reynolds, 1989). Group 3 I-T-S-V patterns (x14, x15, 86, 89, 101) are different mainly because the content of illite layers increases (0.84–0.86) and the illite layer thickness increases to 10.05 Å (Figure 4).

Comparison of the amount of non-expandable illite layers in I-S-V of the studied samples (Table 1) with those presented by Lindgreen *et al.* (1991, Table 1) shows that for some samples the proportion of illite layers determined by Lindgreen *et al.* is greater mainly because they simulated XRD patterns in terms of a two-component I-S model and therefore the presence of 13 Å vermiculite layers in the actual I-S-V structure lead to overestimation of the content of illite layers. Note that transition from group 1 to group 3 is accompanied by a decrease in the amount of K in illite-like interlayers from 0.75 to 0.5 atoms per $O_{10}(OH)_2$. Both the increase in the illite-layer thickness and the decrease in the amount of K indicate the presence of NH_4 in illite-like interlayers. The I-S-V are, in fact, the mixed-layer four-component system I-T-S-V (Drits *et al.*, 1997b), because the non-expandable layers in the mixed-layer phases are 9.98 Å illite and 10.33–10.35 Å tobelite layers. Figure 5 compares the experimental XRD patterns with those calculated for I-T-S-V models. It is remarkable that the amounts of tobelite layers determined by the simulation

https://doi.org/10.1346/000986002761002702 Published online by Cambridge University Press

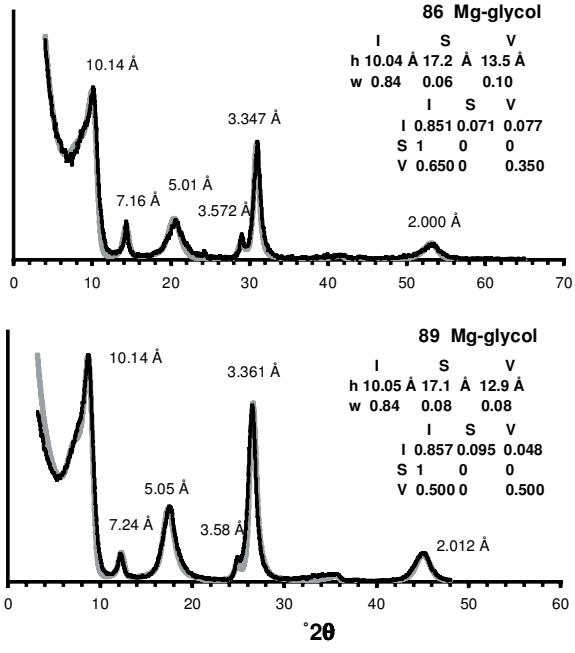

Figure 4. X-ray diffraction patterns of specimens of samples 86 and 89 of group 3 fitted with three components (I, S, V). Explanation and symbols as for Figure 2. The reflections with spacings of ~7.2 Å and 3.5 Å correspond to a kaolinitic phase. For sample 86: CoKα radiation, and for sample 89: CuKα radiation.

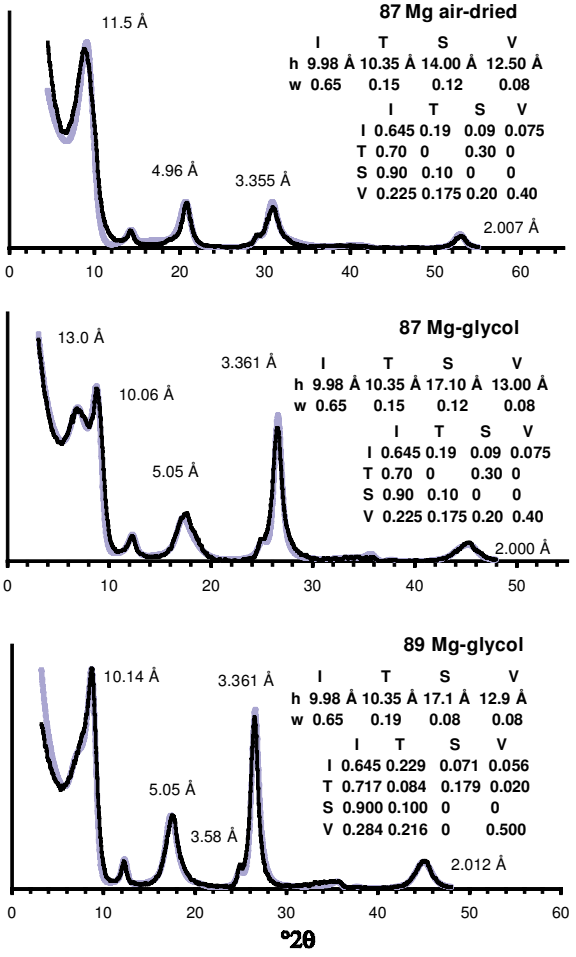

Figure 5. X-ray diffraction patterns of specimens of samples 87 of group 2 and 89 of group 3 fitted with four components (I, T, S, V). For sample 87, the diffraction patterns for both the air-dried and the glycolated specimens are shown. Explanation and symbols as for Figure 2. The patterns from two different Mg-saturated specimens, one air-dried (CoKα radiation) and one intercalated with ethylene glycol (CuKα radiation), demonstrate that one structural model fits all the totally different patterns obtained by different treatments of one sample. The reflections with spacings of 7.23 Å and 3.55 Å correspond to a kaolinitic phase. 87 Mg air-dried: CoKα radiation, 87 Mg-glycol and 89 Mg-glycol: CuKα radiation.

coincides with those determined independently for the same samples using the technique of Drits *et al.* (1997a). For example, both the simulation (Figure 5) and the basal reflection width ratios (Table 4 in Drits *et al.* (1997a)) gave the same content of tobelite layers in I-T-S-V phase, 0.15 and 0.19 for samples 87 and 89, respectively.

The conjunction probability parameters for the three- and four-component models for samples 87 and 89 are shown by the matrices presented in Figures 3, 4 and 5. From these matrices, the layer pair probabilities $w_{ij} = w_i p_{ij}$ (i, j = I, T, S, V) in the four-component model and the probabilities $w_{ij} = w_i p_{ij}$ (i, j = I, S, V) of the three-component model are calculated and new matrices consisting of w_{ij} may be written as:

	I	T	S	V			I	S	V	
I	0.419	0.124	0.059	0.048		I	0.648	0.104	0.048	
T	0.105	0	0.045	0	⇌	S	0.12	0	0	sample 87
S	0.108	0.012	0	0		V	0.032	0.016	0.032	
V	0.018	0.014	0.016	0.032						

	I	T	S	V			I	S	V	
I	0.411	0.149	0.046	0.044		I	0.712	0.08	0.048	
T	0.136	0.016	0.034	0.004	⇌	S	0.08	0	0	sample 89
S	0.072	0.008	0	0		V	0.048	0	0.032	
V	0.031	0.017	0	0.032						

https://doi.org/10.1346/000986002761002702 Published online by Cambridge University Press

Table 1. Number of the layer types in I-T-S-V determined from simulation of XRD patterns.

Sample	Well	Depth (m)	w_{I+T}[1]	w_T[2]	w_I[3]	w_{S+V}[4]	w_S[5]	w_V[6]
Group 1								
x3	SE Igor 1	2502	0.75	0.08	0.67	0.25	0.20	0.05
80	U1	2542	0.70	0.05	0.65	0.30	–	–
82	U1	2899	0.73	0.07	0.66	0.27	0.20	0.07
83	M8	2368	0.66	0.03	0.63	0.34	0.31	0.03
95	Haldager 1	1042	0.69	0.06	0.63	0.31	0.25	0.06
99	Frederikshavn 1	649	0.70	0.06	0.64	0.30	–	–
112	E1	2983	0.68	0.06	0.62	0.32	0.27	0.05
Group 2								
x1	E Rosa 3/3A	1520	0.85	0.03	0.82	0.15	0.05	0.10
x5	N Jens 1	2961	0.82	0.18	0.64	0.18	0.09	0.09
x6	N Jens 1	2965	0.83	0.20	0.63	0.17	0.09	0.08
113	E1	3938	0.82	0.17	0.65	0.18	0.09	0.09
x12	Iris 1	3966	0.82	0.20	0.62	0.18	0.09	0.09
x13	Iris 1	4168	0.82	0.21	0.61	0.18	0.09	0.09
x17	Jeppe 1	4418	0.78	0.09	0.69	0.22	0.10	0.12
87	2/11-1	4548	0.80	0.16	0.64	0.20	0.12	0.08
Group 3								
x14	Iris 1	4174	0.85	0.22	0.63	0.15	–	–
x15	Iris 1	4269	0.85	0.18	0.67	0.15	–	–
86	2/11-1	3877	0.84	0.20	0.64	0.16	0.06	0.10
89	2/7-3	3789	0.84	0.19	0.65	0.16	0.08	0.08
101	I1	3908	0.85	0.17	0.65	0.15	–	–

[1] Number of non-expandable interlayers
[2] Number of tobelite interlayers
[3] Number of illite interlayers
[4] Number of expandable interlayers
[5] Number of smectite interlayers
[6] Number of vermiculite interlayers

For both samples the parameter sums $w_{II} + w_{IT} + w_{TI} + w_{TT}$, $w_{IS} + w_{TS}$, $w_{IV} + w_{TV}$, $w_{SI} + w_{ST}$ and $w_{VI} + w_{VT}$ for the four-component I-T-S-V model are equal to the sums w_{II}, w_{IS}, w_{IV}, w_{SI} and w_{VI} for the three-component I-S-V model. Note that for the four-component models of both samples $w_{IT} \approx w_{TI}$, $w_{TS} > w_{ST}$, whereas the w_{TT}, w_{TV}, w_{SS}, w_{SV} and w_{VS} are either very low or equal to zero. It should be noted that simulation of the experimental XRD patterns was performed for the I-S-V and I-T-S-V without illite as an individual phase.

Thermally evolved water

The step-heating EWA curves (Figure 6) of most studied samples are quite similar and have one strong and broad dehydroxylation maximum at 510–550°C. However, for some samples (x3, x5, 89) the step-heating curves contain additional maxima at temperatures >600°C. The relative area of the high-temperature dehydroxylation calculated as the ratio of this area to the sum of the high- and low-temperature maxima was <0.04 for most samples, but was 0.15 for some of them (Table 2).

Fixed NH_4 content

Infrared spectra of samples from groups 2 and 3 have an intense absorption band near 1430 cm^{-1} (Figure 7) corresponding to NH_4 absorption maxima in tobelites (Vedder, 1965; Yamamoto and Nakahira, 1966; Karyakin *et al.*, 1973; Higashi, 1978; Juster *et al.*, 1987). For group 1, the spectra either have rather weak or no maxima in this region.

For the IR spectrum of sample 89, the decomposition in the region of the OH-stretching vibration into individual bands of the OH, H and NH_4 vibrations is shown in Figure 8. The areas of the bands corresponding to the OH and NH_4 (at 1430 cm^{-1}) vibrations (Figures 7 and 8) were transformed to optical densities of I_{OH} and I_{NH_4}, respectively. The I_{NH_4}/I_{OH} values and the amount of NH_4 taken from Table 1 in Lindgreen (1994) and from Table 4 in Drits *et al.* (1997a) are almost the same (Table 3) showing that the technique is accurate for determination of NH_4 in the NH_4-bearing mixed-layer minerals.

Table 2. EWA analysis, stepwise heating.

Sample	T(°C)	Area (%)	T(°C)	Area (%)
x3	510	85	600	15
x1	503	100		
x5	506	84	596	16
x13	496	100		
x14	503	100		
89	500	96	620	4

https://doi.org/10.1346/000986002761002702 Published online by Cambridge University Press

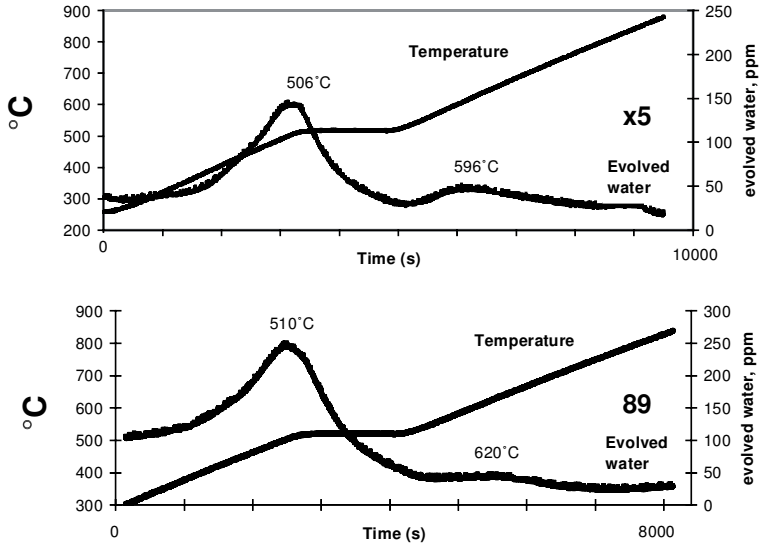

Figure 6. Evolved water curves obtained by step-wise heating for sample x5 of group 2 and sample 89 of group 3.

Mössbauer spectra decomposition

The Mössbauer spectra have been decomposed into two doublets for Fe^{3+} and Fe^{2+}, respectively. Parameters of the inner doublets are reflected in visual splitting of the spectra and vary from 0.58 to 0.63 mm/s, typical of Fe^{3+}-bearing dioctahedral layer silicates (Johnston and Cardile, 1987). The ratios of areas corresponding to the Fe^{3+} and Fe^{2+} doublets are used for calculation of the I-T-S-V structural formulae.

Average structural formulae for the I-T-S-V

For the cuttings samples, Lindgreen *et al.* (1991) determined total chemical composition, Si/^{IV}Al and ^{IV}Al/^{VI}Al values using AAS and NMR methods but not accurate structural formulae for the I-S-V phase because of the kaolinitic phase content. Using the data of Lindgreen *et al.* (1991) and following the procedure described above, we have calculated the average formulae for the cuttings samples and the proportions of I-S-V and kaolinite (Table 4). The fact that Si/^{IV}Al and ^{IV}Al/^{VI}Al values calculated from the average formulae and measured by NMR almost coincide (Table 4) shows that both techniques provide reliable results.

Table 5 contains the structural formulae of I-T-S-V calculated from equations 2 and 3. In all samples the I-T-S-V contain almost the same amount of fixed interlayer K

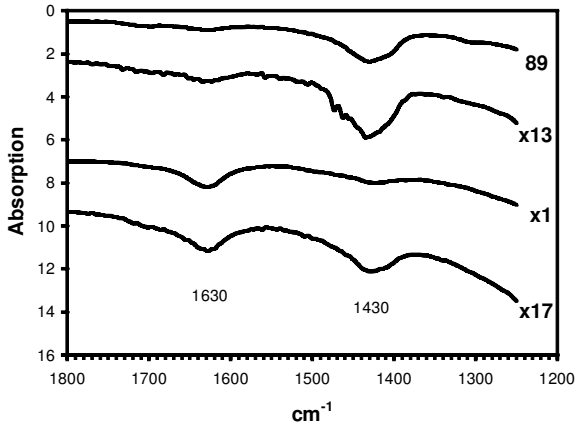

Figure 7. Sections of the IR spectra containing the NH_4 (1410–1440 cm^{-1}) band for K-saturated and heated (150°C) samples x1, x13 and x17 of group 2 and 89 of group 3.

Table 3. Relationship between I_{NH_4}/I_{OH} and NH_4 content in the I-T-S-V.

Sample	I_{NH_4}/I_{OH} [1]	c_{NH_4} [2]	c_{NH_4} [3]	w_T [4]	$2c_{NH_4}$ [5]
Group 1					
x3	0.06	0.07	0.10	0.08	0.08
82	0.07	0.08	0.07	–	0.07
95	0.04	–	0.06	0.08	0.06
Group 2					
x1	0.04	0.03	0.03	0.00	0.03
x12	0.20	0.20	0.22	0.19	0.20
x13	0.21	0.21	0.22	0.19	0.21
x17	0.08	0.10	0.10	0.08	0.09
87	0.18	–	0.15	0.15	0.16
Group 3					
89	0.18	0.22	0.18	0.17	0.19

[1] Ratio between IR optical densities of the NH_4 band at 1430 cm^{-1} and the OH band at 3631 cm^{-1}
[2] Data by the isotopic dilution method (Lindgreen, 1991)
[3] Data from 005 reflection positions of K-saturated and dehydrated I-T-S-V (Table 4, Drits *et al.*, 1997b)
[4] Data from the FWHH(005)/FWHH(002) values (Table 4, Drits *et al.*, 1997b)
[5] Average of the four c_{NH_4} determinations

https://doi.org/10.1346/000986002761002702 Published online by Cambridge University Press

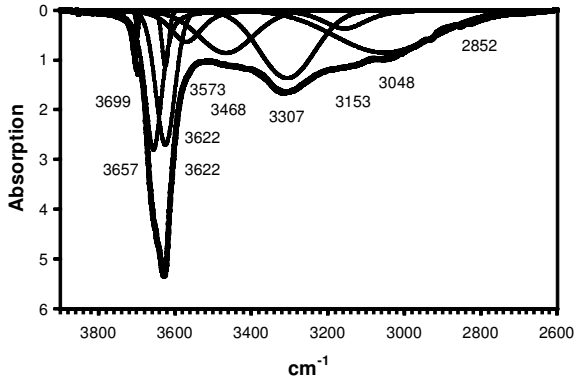

Figure 8. Decomposition into individual bands for sample 89 (K-saturated and heated to 150°C) of the complex maximum of the IR spectrum in the stretching region. The bands at 3657, 3622 and 3573 cm^{-1} correspond to OH, those at at 3468 and 3153 cm^{-1} to water molecule vibration and those at 3307 and 3048 cm^{-1} to NH_4. The band at 3699 cm^{-1} is due to kaolinite.

(0.38 ± 0.02) whereas the NH_4 content increases from 0 to 0.22 cations per $O_{10}(OH)_2$. The increase of NH_4 is accompanied by a significant increase of Al in tetrahedral sheets. For example, for samples taken from the shallow depth (70, 80, 82, 83), the amount of ^{IV}Al per $O_{10}(OH)_2$ varies from 0.33 to 0.40 atoms whereas for diagenetically transformed samples the ^{IV}Al content increases to 0.54–0.66 atoms per $O_{10}(OH)_2$. The octahedral cation content of the 2:1 layers also changes significantly during diagenesis. For example, the ^{VI}Al content increases from 1.31 per $O_{10}(OH)_2$ for sample 70 to 1.69 for sample 89 whereas the Fe and Mg contents decrease from 0.35 to 0.16 and from 0.34 to 0.14, respectively.

Mean number of layers in the CSDs and illite fundamental particles

Table 6 contains the mean numbers of layers in the CSDs (N) determined by the 001 reflection profile analysis of K-saturated and dehydrated samples and the mean number of 2:1 layers in illite fundamental particles ($\bar{n}$) in the I-T-S-V calculated from equation 4. With a decrease of the expandable interlayers, the values of N increase from 5.3 to 6.4 layers and the values of $\bar{n}$ from 2.2 to 3.4 layers (Table 6).

DISCUSSION

NH_4- and K-bearing non-expandable interlayers

For I-S a quantitative determination of content and distribution of NH_4 by diffraction methods is difficult because different proportions and distributions of layer types modify the positions, intensity and profile of basal reflections more strongly than the presence of NH_4. However, diffraction sensitivity to structural NH_4 increases significantly if the samples are saturated with K and dehydrated because then the thickness of the K-saturated expandable layers will be equal to the thickness of illite layers and the I-S thus becomes a two-component structure of interstratified 9.98 Å K-containing and 10.33 Å NH_4-containing mica layers.

In NH_4-bearing I-S-V, K and NH_4 in mica interlayers may be distributed as follows: (1) homogeneously, *i.e.* interlayers have identical amounts of (K + NH_4) and NH_4/K ratios; (2) interlayers contain either K or NH_4; or (3) interlayers have different NH_4/K ratios. For K-saturated and dehydrated samples, the amount of fixed NH_4 per $O_{10}(OH)_2$, c_{NH_4}, is determined by the $d(005)$ value and is independent of the K and NH_4 distribution, which is determined by the ratio between full width at half heights (FWHH) of 00l reflections. In particular, FWHH(005)/FWHH(002) determines the content of NH_4-bearing 10.33 Å layers, w_{NH_4}, in the mixed-layer structure of type 2. It must be emphasized that the functional relationships between c_{NH_4} and $d(005)$ and between w_{NH_4} and FWHH(005)/FWHH(002) are independent. Therefore, samples having equal amounts of K

Table 4. Averaged cation composition of the cutting samples (per $O_{10}(OH)_{(8-6p)}$) and Si/^{IV}Al and ^{IV}Al/^{VI}Al calculated from the formulae and determined by NMR.

Sample	Si	^{IV}Al	^{VI}Al	Fe^{3+}	Fe^{2+}	Mg	Σ_{oct}	p[1]	K	NH_4	Na	Ca	Si/^{IV}Al (2)	Si/^{IV}Al (3)	^{IV}Al/^{VI}Al (2)	^{IV}Al/^{VI}Al (3)
70[4]	3.70	0.30	1.60	0.28	0.07	0.27	2.22	0.89	0.33	0	0.24	0.03	12.5	11.7	0.17	0.18
80	3.62	0.38	1.51	0.30	0.05	0.28	2.14	0.93	0.35	0.05	0.24	0.01	9.6	9.6	0.25	0.24
82	3.67	0.33	1.63	0.23	0.05	0.30	2.21	0.89	0.36	0.08	0.24	0.01	11.0	11.0	0.20	0.21
83	3.67	0.33	1.57	0.25	0.04	0.30	2.16	0.92	0.35	0.04	0.26	0.02	11.2	11.2	0.21	0.21
113	3.56	0.44	1.62	0.24	0.05	0.23	2.14	0.93	0.38	x[6]	0.28-x	0.02	8.0	7.5	0.27	0.27
79[5]	3.52	0.48	1.73	0.22	0.04	0.23	2.22	0.89	0.35	0.13	0.25	0.01	7.3	7.3	0.28	0.28
87	3.36	0.54	1.55	0.21	0.07	0.20	2.00	0.98	0.37	0.16	0.19	0.02	6.4	6.4	0.35	0.35
86	3.43	0.57	1.64	0.16	0.04	0.16	2.03	1.00	0.36	0.21	0.21	0	6.0	5.8	0.35	0.35
89	3.35	0.65	1.69	0.12	0.04	0.14	2.00	1.00	0.40	0.22	0.15	0.03	5.1	5.0	0.38	0.38

[1] Proportion of the I-S-V or I-T-S-V phase
(2) From chemical formulae
(3) From NMR
[4] Well G2, 2609 m
[5] Well Lulu 1, 3420 m
[6] not determined

https://doi.org/10.1346/000986002761002702 Published online by Cambridge University Press

Table 5. Structural formulae for the I-T-S-V.

Sample	Si	^{IV}Al	^{VI}Al	Fe^{3+}	Fe^{2+}	Mg	K	NH_4	Na	Ca	O	(OH)
70	3.67	0.33	1.31	0.31	0.05	0.33	0.37	0	0.27	0.04	10	2
80	3.59	0.41	1.32	0.33	0.05	0.30	0.38	0.05	0.32	0.02	10	2
82	3.63	0.37	1.35	0.25	0.06	0.34	0.40	0.09	0.26	0.01	10	2
83	3.64	0.36	1.36	0.28	0.04	0.32	0.38	0.04	0.29	0.02	10	2
113	3.53	0.47	1.46	0.25	0.05	0.24	0.40	x[1]	0.31-x	0.02	10	2
79	3.46	0.54	1.45	0.25	0.04	0.26	0.39	0.13	0.28	0.01	10	2
87	3.45	0.55	1.51	0.22	0.07	0.20	0.38	0.16	0.23	0.02	10	2
86	3.43	0.57	1.64	0.16	0.04	0.16	0.36	0.21	0.19	0	10	2
89	3.35	0.65	1.69	0.12	0.04	0.14	0.40	0.22	0.15	0.03	10	2

[1] not determined

and NH_4 and the same $d(00l)$ values may have different $00l$ basal reflection widths and samples having equal basal reflection widths may have different K and NH_4 contents. For the studied mixed-layer phases, the c_{NH_4} and w_{NH_4} values determined from the $d(005)$ and FWHH(005)/FWHH(002), respectively, are almost the same (Drits *et al.*, 1997a) and coincide with the content of fixed NH_4 per $O_{10}(OH)_2$ determined by the accurate isotopic dilution method (Lindgreen, 1994). These results demonstrate that, first, the K-saturated and dehydrated phase has a mixed-layer structure consisting of 9.98 Å and 10.33 Å layers, and, second, the diagenetically transformed phase consists of interstratified illite, tobelite, smectite and vermiculite. Simulation of the experimental XRD patterns using the I-T-S-V model confirms the second conclusion and shows a tobelite content equal to c_{NH_4} and w_{NH_4}. The direct link between total amount of NH_4 and content of tobelite layers in the NH_4-bearing I-S studied follows from the relationship between I_{NH_4}/I_{OH} and w_T (Figure 9). The IR band at 1430 cm^{-1} is sensitive to the total amount of NH_4, independent of distribution of K and NH_4 over non-expandable mica interlayers in NH_4-bearing I-S. The fact that I_{NH_4} normalized for the number of OH groups in the unit-cell (I_{OH}) is proportional to the amount of tobelite layers determined from the FWHH(005)/FWHH(002) values is additional evidence for separate distribution of K and NH_4 among mica interlayers.

The total content of non-expandable mica interlayers, $w_{I+'T}$, determined by the experimental XRD simulation and the amount of tobelite interlayers, w_T, determined from the basal reflection positions and widths are compared in Table 1. The difference between these values is equal to the content of illite interlayers, w_I, in the I-T-S-V studied. Table 1 shows that w_I is equal to (0.65 ± 0.05) independent of sample location, burial depth and temperature. It is remarkable that according to the structural formulae (Table 4) the I-T-S-V contain almost the same amount of K per $O_{10}(OH)_2$ (0.38 ± 0.02). This means that diagenesis does not change illite interlayers. Accordingly, diagenetic trans-

Table 6. Number of layers in CSDs and in fundamental particles and content of K per $O_{10}(OH)_2$ in the I-T-S-V.

Sample	N[1]	w_{S+V}[2]	$\bar{n}$[3]	w_T[4]	w_I[5]	K[6] $c_K = 0.75$	K[7] $c_K = 0.90$
x3	5.9	0.25	2.65	0.08	0.67	0.41	0.49
82	5.9	0.30	2.39	0.07	0.63	0.39	0.47
95	5.3	0.31	2.27	0.06	0.63	0.38	0.45
112	5.5	0.32	2.25	0.06	0.62	0.38	0.45
79	5.7		2.3				
x13	6.4	0.20	3.07	0.20	0.60	0.38	0.45
x17	6.0	0.20	3.0	0.09	0.71	0.44	0.53
87	6.4	0.20	3.07	0.16	0.64	0.40	0.48
89	6.4	0.16	3.43	0.19	0.65	0.41	0.49

[1] Mean number of layers in CSDs
[2] Total expandability
[3] Mean number of layers in illite fundamental particles
[4] Number of tobelite layers
[5] Number of illite layers
[6] Amount of K in I-T-S-V calculated from equations 5 and 6 assuming 0.75 K per $O_{10}(OH)_2$ of illite
[7] Amount of K in I-T-S-V calculated from equations 5 and 6 assuming 0.90 K per $O_{10}(OH)_2$ of illite

https://doi.org/10.1346/000986002761002702 Published online by Cambridge University Press

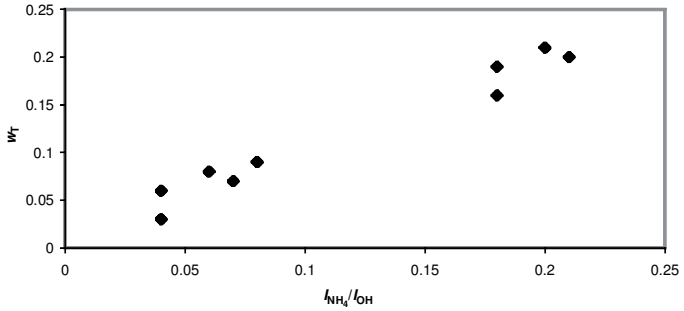

Figure 9. Content of tobelite layers, w_T, in I-T-S-V *vs*. the ratio between IR optical densities, I_{NH_4}/I_{OH}, of the NH_4 band at 1430 and the OH band at 3631 cm^{-1}.

formation of I-S-V in the Upper Jurassic oil-source rock is accompanied not by an illitization of smectite involving fixation of K as generally accepted but solely by a formation of tobelite layers due to fixation of NH_4 in former smectite and/or vermiculite interlayers.

Tobelitization of smectite is a characteristic feature of the I-T-S formed simultaneously with oil generation. In particular, our investigation of samples from Cambrian black shales has shown that the I-S and I-T-S have the same K content and increase of layer charge because the increase of ^{IV}Al is compensated by NH_4 (Lindgreen *et al*., 2000). As a consequence, the K content in mixed-layers from oil-source rocks cannot be used to indicate the increase in amount of mica layers, because the newly formed mica layers are in fact tobelite layers. Furthermore, conventional K/Ar dating cannot be applied to investigate the timing of diagenesis but represents mainly the time of formation of the initial or mica material (later transformed to I-S-V by weathering) in the parent rock.

An exception from the tobelitization is, however, sample x1 taken from the East Rosa 3/3A well at 1520 m depth. For this sample, the amount of NH_4 determined by the isotopic dilution method (Lindgreen, 1994) and from the positions and widths of basal reflection (Drits *et al*., 1997a) does not exceed 0.03 per $O_{10}(OH)_2$. However, the experimental XRD pattern corresponds to group 2 and an I-S-V phase containing the largest amount of illite layers (0.86), I and S being distributed with maximum possible degree of ordering at R = 1 and V layers have a tendency to segregation. This sample is special in the way that the Upper Jurassic shale in this well is comparatively thin (10 m) and that it is positioned immediately above a Zechstein salt structure and below a thin Upper Cretaceous chalk (89 m). This indicates that the salt movement started in Cretaceous time and that the Upper Jurassic shale was never buried to a depth sufficient to initiate oil formation or diagenesis of smectite layers. Instead, it is probable that salt solutions have migrated from the Zechstein salt through the thin Upper Jurassic shale, having supplied sufficient heat to cause tetrahedral substitution of smectite transforming it into illite and supplying the K for formation of illite layers. This agrees with the finding that only a little soluble NH_4 is present in the shale compared to K, any NH_4 formed during transformation of organic matter probably having been flushed out of the shale by the migrating solutions. Previously, such migrating solutions were indicated by Jensenius (1987) who investigated fluid inclusions in the Upper Cretaceous chalk of the North Sea Skjold oil field and found indications that hot water solutions (87–112°C, as indicated from inclusions) from deeper layers had migrated through the chalk.

Fixed K content in illite interlayers of the I-T-S-V

Meunier and Velde (1989) and Środoń *et al.* (1992) suggested that the fixed K^+ content in illite interlayers, c_K, of I-S is 0.9 per $O_{10}(OH)_2$. Simulation of the XRD patterns of the I-S-V and I-T-S-V from the Upper Jurassic shales performed by Drits *et al.* (1997b) and in the present study has shown that 0.75 K per $O_{10}(OH)_2$ provided much better agreement between the experimental and calculated XRD patterns than 0.9 K per $O_{10}(OH)_2$. The 0.75 K is supported by calculations of the amount of interlayer K from the mean number of layers in illite fundamental particles (Table 6). The number of illite interlayers in illite fundamental particles is $\bar{n}-1$ and the K content per $O_{10}(OH)_2$ in the structural formulae of the I-S-V having only illite interlayers is

$$(\bar{n} - 1)c_K/\bar{n} \quad (5)$$

If the non-expandable mica interlayers are illite, w_I, and tobelite, w_T, then the amount of K per $O_{10}(OH)_2$ in the I-T-S-V should be equal to

$$c_K w_I(\bar{n} - 1)/[(w_I + w_T)\bar{n}] \quad (6)$$

The K contents calculated for c_K = 0.75 and 0.90 are given in Table 6. The number of K calculated for c_K = 0.75 is, except for sample 17, practically equal to the number determined from the structural formulae (Tables 4 and 5). The same value, 0.75 K per $O_{10}(OH)_2$, was previously determined for illite interlayers in I-S and I-T-S from Cambrian Black shale of the Baltic area (Lindgreen *et al*., 2000). This coincidence, obtained by two independent methods is additional evidence that tobelitization of the expandable layers is not accompanied by K fixation.

https://doi.org/10.1346/000986002761002702 Published online by Cambridge University Press

Structural mechanism of an I-T-S-V transformation

Several main structural mechanisms of transformation have been proposed for the smectite illitization: solid state, neoformation and Ostwald ripening (Altaner and Ylagan, 1997; Środoń *et al.*, 2000). Each of these reactions may result in fixation of NH_4 in newly formed mica layers. However, only the solid-state transformation can explain the constant amount of pure illite layers when the amount of mica layers increases due to smectite tobelitization.

Neoformation and recrystallization as well as Ostwald ripening are accompanied by an increase of particle size and, in addition, the newly formed particles show well-developed crystal faces. In contrast, the solid-state reaction does not change the size and the morphology of the particles significantly. For the I-S-V from the North Sea area, atomic force microscopy (Figure 10) shows that the size and the shape of the individual particles do not change significantly with degree of diagenesis and that crystals with well-developed faces are not appearing in the samples transformed during diagenesis, two facts that support the conclusion of a solid-state transformation. An increase in the mean number of layers in CSDs from 5.3–5.9 for I-S-V from the Danish Subbasin and the shallow Central Trough samples to 6.0–6.4 for I-T-S-V from the diagenetically transformed central Trough shales takes place because the transformation of former smectite interlayers into tobelite is probably accompanied by increasing numbers of layers parallel to each other.

The tobelitization reaction may be imaged as a sequential substitution of a smectite by a tobelite interlayer. In the detrital mixed-layer crystals, NH_4 and Al migrate from solution to the interlayer space of smectite interlayers. Substitution of Si for Al then increases the negative charge of the tetrahedral sheets in the 2:1 layers of smectite. Direct evidence of the increase of tetrahedral Al in the 2:1 layers in the I-S-V and I-T-S-V with increasing temperature and burial depth has been obtained by solid-state high-resolution MAS NMR spectroscopy (Lindgreen *et al.*, 1991) and is seen in the structural formulae (Table 5). This increase in tetrahedral charge combined with fixation of dehydrated NH_4^+ between these illite tetrahedral sheets results in formation of tobelite layers. Adjacent tetrahedral sheets of smectite are thus transformed into vermiculite tetrahedral sheets and further or directly into illite tetrahedral sheets. In addition to substitution of Si for Al, the transformation is accompanied by significant modification of octahedral cation composition of the 2:1 layers due to a substitution of Fe and Mg for Al. The migration of octahedral cations may take place through smectite interlayers without disturbing the illite interlayers. This is due to the fact that the illite fundamental particles in I-S-V prior to tobelitization are very thin having mean numbers of layers equal to 2.2–2.4 (Table 6).

Selective sorption and fixation of NH_4

Why is NH_4^+ but not K^+ fixed in newly formed mica layers? Analysis of soluble plus exchangeable NH_4 and K in the core samples of the Central Trough shows that the amount of soluble K decreases with depth of the sample whereas the amount of NH_4 increases (Lindgreen, 1994). These results correlate with the observed increase of fixed NH_4 in the studied I-T-S-V (Table 1). However, in the Central Trough, concentrations

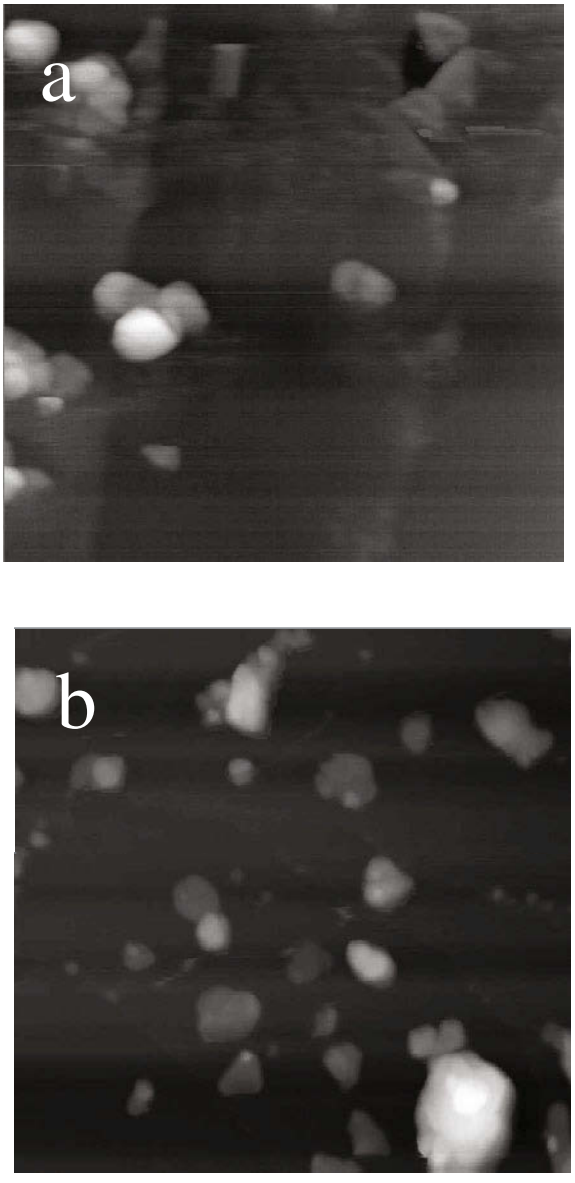

Figure 10. Atomic force microscopy images of I-S fractions deposited on graphite. 0.186 nN, non-contact mode. Mean value filter applied. (a) Sample 112; (b) Sample 89.

https://doi.org/10.1346/000986002761002702 Published online by Cambridge University Press

of soluble plus exchangeable K, 0.8 to 7.6 meq/100 g, is several times greater than for NH_4, 0.07 to 0.64. Thus, in spite of the predominance of K in solution, a selective absorption and fixation of NH_4 in the former smectite interlayers takes place. This preferential absorption of NH_4^+ in neoformed mica interlayers may be due to the different reaction of different cations to increasing layer charge (Eberl, 1986; Lindgreen, 1994). For a given layer charge, the larger cation in the dehydrated state is more easily dehydrated. At low layer charge all cations are hydrated. With increasing interlayer charge due to substitution of Si for Al in smectite tetrahedral sheets, NH_4 is dehydrated and fixed first because of its larger size (1.43 Å) compared to K (1.33 Å) and possibly also because of the formation of hydrogen bonds with oxygen atoms in the interlayer surface and because of the cation demixing effect (Gaultier and Mamy, 1979, 1982).

Analysis of the data presented by Lindgreen (1994) for soluble plus exchangeable ($c^S_{NH_4}$) and fixed ($c^F_{NH_4}$) NH_4 content for the studied samples shows that these values are interrelated: the higher the value of $c^S_{NH_4}$, the higher the value of $c^F_{NH_4}$ (Figure 11). An exception is sample 112 of group 1 taken from well E1 at 2984 m depth which has the highest soluble NH_4 content (0.56 meq/100 g) but the I-T-S-V phase contains only 0.06 of NH_4 per $O_{10}(OH)_2$ (Figure 11). The sample is at the onset of oil generation (Thomsen *et al.*, 1983); therefore this NH_4 probably originates from deeper layers and has migrated through the shale to 2984 m depth. Sample 113 from the same well at 3938 m contains 0.17 tobelite interlayers (Table 1). Accordingly, fixation of NH_3 at temperatures lower than maximum oil generation does not take place, because of the lack of increase in tetrahedral charge. The link between tobelitization and maximum oil generation is probably a link between breaking of bonds in organic material (*e.g.* C–C and C–N bonds) and, at the same temperature, breaking of Si–O bonds and formation of Al–O bonds, and, with the resulting increased tetrahedral charge, fixation of released NH_3.

Source areas and parent material for the I-S-V

Hansen and Lindgreen (1989), Lindgreen (1991) and Drits *et al.* (1997b) showed that I-S-V samples of group 1 have detrital origin, and have not been transformed significantly by diagenesis. The mixed-layer minerals probably formed during weathering of illite and were transported from the Fennoscandian Shield. The I-S-V of group 1 have a significant tendency to segregation which is quite unusual for diagenetically transformed I-S. This tendency to segregation of the layer types formed during illite weathering was probably inherited in the I-S-V. In addition, the I-S-V is associated with mixed-layer kaolinite-illite-vermiculite which probably also formed through weathering of illite (Drits *et al.*, 1997b).

Tsipursky and Drits (1984) showed that normally Al-rich smectites consist of *cis*-vacant (*cv*) and illites of

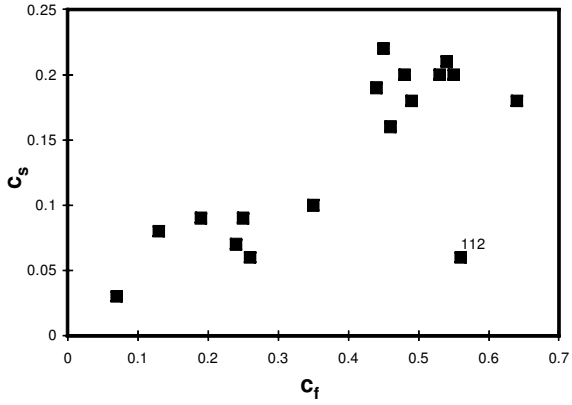

Figure 11. Amount of soluble plus exchangeable NH_4, c(s), in samples from cores *vs.* the fixed NH_4 content, c(F), in I-T-S-V in the same samples, with the plot for sample 112 identified. Data from Lindgreen (1994).

trans-vacant (*tv*) 2:1 layers. Accordingly, a formation of illite (*tv*) layers from smectite (*cv*) layers should lead to interstratification of *tv* and *cv* layers in I-S and to an increase in proportion of *tv* 2:1 layers, whereas I-S formed during weathering of illite (*tv*) independent of the layer types should have only *tv* octahedra. Drits *et al.* (1995) showed that *tv* and *cv* 2:1 layers have dehydroxylation temperatures of 500–600°C and 650–750°C, respectively. Therefore, I-S-V formed from smectite should have a DTA-EWA curve with two endothermic peaks corresponding to dehydroxylation of the *tv* and *cv* layers (Drits *et al.*, 1996, 1998b; Cuadros and Altaner, 1998; Lindgreen *et al.*, 2000). In contrast, DTA-EWA curves of I-S-V formed by weathering of illite (*tv*) should have only one dehydroxylation peak below 600°C. For the North Sea I-S-V and I-T-S-V, the main thermal decomposition occurs below 550°C for samples of groups 1, 2 and 3 (Table 2), and therefore the North Sea I-S-V and I-T-S-V consist mainly of *tv* layers. Some samples contain a small amount of *cv* layers, but this content does not correlate with the amount of non-expandable mica layers or with the degree of diagenesis. The predominance of *tv* layers in the studied I-S-V and I-T-S-V is in accord with the fact that these minerals formed by weathering of illite.

The fact that all the mixed-layer minerals studied, independent of their location and burial depth, contain the same amount of pure illite layers (Table 1) finally confirms that the I-S-V and I-T-S-V have formed from the same parent material and have the same source area.

Oil generation and tobelite transformation windows

In the Norwegian-Danish Basin, the amount of uplift during the Tertiary was ~1 km. If the geothermal gradient was ~25°C/km (Thomsen *et al.*, 1983), the present-day temperature of 24–51°C had reached a maximum of 50–75°C. Except for sample x1, samples from the Central Trough are experiencing their maximum temperature during burial history at present,

https://doi.org/10.1346/000986002761002702 Published online by Cambridge University Press

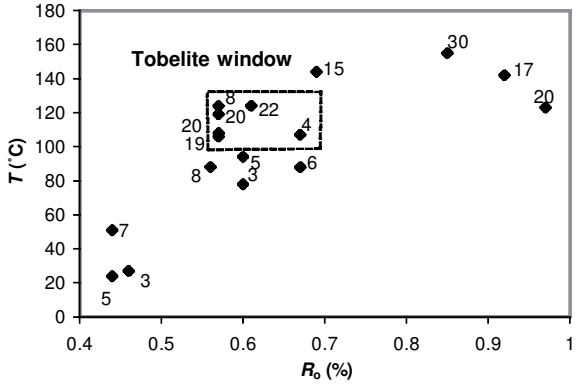

Figure 12. Relationship between proportion of tobelite layers, w_T, formation temperature of the samples, T, and vitrinite reflectance values, R_o, for North Sea and Norwegian–Danish basin I-T-S-V minerals. Labels for each point correspond to the w_T value for the I-T-S-V. The tobelite window is limited by the vitrinite reflectance values $R_o \approx 0.55–0.7\%$.

because of a large subsidence during the Tertiary. Figure 12 shows how the content of newly formed tobelite layers in I-T-S-V depends on the formation temperature, T (T. Bidstrup, pers. comm.; Lindgreen, 1991) and the vitrinite reflectance values, R_o (Thomsen *et al.*, 1983; Lindgreen, 1991; C. Guvad, pers. comm.). The I-S-V of samples from the Norwegian–Danish Basin and from shallow depth (<3000 m) in the Central Trough (with T <100°C and R_o <0.70%) contain <0.10 tobelite layers (Figure 12, Table 1). At greater depths in the Central Trough the number of tobelite layers is generally much larger, for $0.55 < R_o < 1.0\%$ and $110 < T < 140$°C the number of tobelite layers is 0.15–0.22 (Table 1).

Before oil generation, the I-S-V from the Central Trough had a limited number of expandable interlayers (S+V) available for tobelitization (0.30–0.35, Table 1). Maximum oil generation and expulsion in the Central Trough took place at vitrinite reflectance values of 0.6–0.7 R_o (Thomsen *et al.*, 1983), the stage at which maximum release of NH_4 during the generation process occurs (Hunt, 1979; Barth *et al.*, 1996). At this stage (at $T \approx 100–120$°C) 50–70% of the expandable interlayers have been transformed into tobelite interlayers (Figure 12). Thus, once the shale has passed into the stage that we call the 'tobelite window', oil generation and expulsion is accompanied by intense tobelitization of previously expandable interlayers. This conclusion is in agreement with the observed relationship between the contents of soluble and fixed NH_4 (Figure 11). With further increasing temperatures and vitrinite reflectance values, the tobelite layer formation decreases or even ceases, probably because the amount of available NH_4 in solution decreases with increasing R_o. The 'oil window' for oil generation in different source rocks corresponds to the vitrinite reflection interval $0.6 < R_o < 1.3$ (Hood *et al.*, 1975; Dow, 1977; Tissot and Welte, 1978; Thomsen *et al.*, 1983) and the temperature interval $80 < T < 140$°C (Hunt, 1979; Barth *et al.*, 1996). The 'tobelitization window' occurs within the 'oil window' and is restricted to the physical-chemical interval where maximum release of NH_4 coincides with intense formation of tobelite layers. For the North Sea oil-source rocks, the tobelitization reaction probably takes place during oil generation and oil expulsion at vitrinite reflectance values of 0.55–0.7 R_o and $T \approx 100–120$°C (Figure 12).

I-T-S-V as an indicator of oil-generating source rocks in sedimentary basins

The tobelitization of smectite in I-S or I-S-V is probably typical for all oil-source rock shales. Therefore the presence of I-T-S or I-T-S-V in sedimentary rocks may be used as independent evidence for oil formation even after migration or thermal decomposition of the oil because once formed, the tobelite interlayers should be stable during low-temperature metamorphism as the release of fixed NH_4 from NH_4-bearing layers takes place above 400°C (Higashi, 1978). The results obtained for I-S from Cambrian Alum black shales of both early diagenetic and anchimetamorphic grade may serve as an example (Lindgreen *et al.*, 2000). In the early diagenetic samples, the I-S is composed of two phases, one of which contains 0.05 and the other 0.25 smectite interlayers. The first highly illitic phase does not change during metamorphism. In the second phase, 0.10–0.18 smectite layers are transformed to tobelite layers. Thus, the number of T layers formed in this phase corresponds to that found in diagenetically transformed I-T-S-V from the Central Trough. It is remarkable that, as for the North Sea I-S-V and I-T-S-V, the number of I layers in the second phase is not changed and all illite interlayers contain 0.75 K per $O_{10}(OH)_2$. As in the case of the North Sea, transition of I-S to I-T-S in the Cambrian shales takes place through a solid-phase transformation. However, in contrast to I-T-S-V from the Central Trough, the I-T-S from Cambrian shale have been transformed strongly during anchimetamorphism. Therefore, organochemical generation parameters cannot be applied. Furthermore, the absence of material from terrestrial vegetation in the Cambrian renders coal petrography useless. However, the presence of a significant amount of I-T-S in the highly transformed Cambrian samples in combination with a high potential for oil generation in early diagenetic samples containing I-S with a small amount (<0.05) of tobelite layers leads to the conclusion that the tobelitization in the Cambrian Alum black shales is related to oil generation which took place before the rocks were transformed during Caledonian folding, including heating to 200°C.

For the North Sea I-S-V and I-T-S-V, structures intermediate between those of group 1 and 2 have not been found. This indicates that the tobelitization is an almost instantaneous process once the temperature for the breaking of Si–O bonds has been reached. Thus, samples 82 and 112 from depths 2899 and 2983 m, respectively, are not tobelitized but samples x5 and x6 from ~2960 m depth are.

https://doi.org/10.1346/000986002761002702 Published online by Cambridge University Press

CONCLUSIONS

For illite-containing mixed-layer minerals from the Upper Jurassic shales of the North Sea, the diagenetic transformation took place simultaneously with oil generation. During burial diagenesis, three-component illite-smectite-vermiculites (I-S-V) were transformed into four-component illite-tobelite-smectite-vermiculites (I-T-S-V) in a diagenetic interval ($110 < T < 140^{\circ}$C, $0.60 < R_o < 0.70\%$) where the maximum release of NH_3 from oil generation in organic matter is accompanied by an intense increase of tobelite layers in I-T-S-V. The amount of pure illite layers (0.65 ± 0.05) as well as the amount of K per $O_{10}(OH)_2$ (0.38 ± 0.02) in the studied I-S-V and I-T-S-V are independent of location, depth and temperature of the rocks. Therefore, the transformation of I-S-V into I-T-S-V, together with an increase in tetrahedral charge by Al for Si substitution, took place exclusively due to selective sorption and fixation of NH_4 cations in former S and V interlayers of the I-S-V. Diagenesis of the oil-source rocks is thus accompanied not by illitization but by tobelitization of expandable layers of the former I-S-V. Independence between the degree of diagenetic transformation on one side and and the amounts of illite layers and of K in I-S-V and I-T-S-V on the other is evidence of a solid-state transformation of the I-S-V into I-T-S-V as well as of a common parent material. In addition, the solid-state transformation is supported by the similar size and shape of the I-S-V and I-T-S-V particles and the common parent material by the vacancy of *trans*-octahedra of the I-S-V 2:1 layers and the tendency to segregation of the layer types in the I-S-V. Thermal stability of the newly formed T layers means that the presence of I-T-S or I-T-S-V in oil-source rocks is independent evidence of oil generation even after migration or thermal decomposition of the oil.

ACKNOWLEDGMENTS

H. Lindgreen, V. Drits, B. Sakharov and A. Salyn thank the Danish Natural Science Research Council for the research grant and V. Drits, B. Sakharov and A. Salyn thank the Russian Foundation of Fundamental Research for partial financial support. We thank D. Christensen, H. C. Ørsted Institute, and C. Guvad, Geological Survey of Denmark and Greenland, for IR spectra, and V. Šucha and P.H. Nadeau for constructive reviews.

REFERENCES

Altaner, S.P. and Ylagan, R.F. (1997) Comparison of structural models of mixed-layer illite/smectite and reaction mechanisms of smectite illitization. *Clays and Clay Minerals*, **45**, 517-533.

Barth, B., Rist, K., Huseby, B. and Ocampo, R. (1996) The distribution of nitrogen between bitumen, water and residue in hydrous pyrolysis of extracted Messel oil shale. *Organic Geochemistry*, **24**, 889–895.

Bell, T.E. (1986) Microstructure in mixed-layer illite/smectite and its relationship to the reaction of smectite to illite. *Clays and Clay Minerals*, **34**, 146–154.

Bernas, B. (1968) A new method for decomposition and comprehensive analysis of silicates by atomic absorption spectroscopy. *Analytical Chemistry*, **40**, 1682–1686.

Bethke, C.M. and Altaner, S.P. (1986) Layer-by-layer mechanism of smectite illitization and application of a new rate law. *Clays and Clay Minerals*, **34**, 136–145.

Cooper, J.E. and Abedin, K.Z. (1981) The relationship between fixed ammonium-nitrogen and potassium in clays from a deep well on the Texas Gulf Coast. *Texas Journal of Science*, **33**, 103–111.

Cuadros, J. and Altaner, S.P. (1998) Compositional and structural features of the octahedral sheet in mixed-layer illite-smectite from bentonites. *European Journal of Mineralogy*, **10**, 111–124.

Dainyak, L.G. and Drits, V.A. (1987) Interpretation of the Mössbauer spectra of nontronite, celadonite, and glauconite. *Clays and Clay Minerals*, **35**, 363–372.

Dow, W.G. (1977) Kerogen studies and geological interpretations. *Journal of Geochemical Exploration*, **7**, 79–99.

Drits, V.A., Besson, G. and Muller, F. (1995) An improved model for structural transformation of heat-treated aluminous dioctahedral 2:1 layer silicates. *Clays and Clay Minerals*, **43**, 718–731.

Drits, V.A., Salyn, A.L. and Šucha, V. (1996) Structural transformations of interstratified illite-smectite from Dolná Ves hydrothermal deposits: dynamics and mechanisms. *Clays and Clay Minerals*, **44**, 181–190.

Drits, V.A., Lindgreen, H. and Salyn, A. (1997a) Determination by X-ray diffraction of content and distribution of fixed ammonium in illite-smectite. Application to North Sea illite-smectites. *American Mineralogist,* **82**, 79–87.

Drits, V.A., Sakharov, B.A., Lindgreen, H. and Salyn, A. (1997b) Sequential structure transformation of illite-smectite-vermiculite during diagenesis of Upper Jurassic shales from the North Sea and Denmark. *Clay Minerals,* **32**, 351–371.

Drits, V.A., Środoń, J. and Eberl, D.D. (1997c) XRD measurement of mean crystallite thickness of illite and illite/smectite: Reappraisal of the Kübler index and the Scherrer equation. *Clays and Clay Minerals,* **45**, 461–475.

Drits, V.A., Eberl, D.D. and Środoń, J. (1998a) XRD measurement of mean thickness, thickness distribution and strain for illite and illite-smectite crystallites by the Bertaut-Warren-Averbach technique. *Clays and Clay Minerals*, **46**, 38–50.

Drits, V.A., Lindgreen, H., Salyn, A.L., Ylagan, R. and McCarty, D.K. (1998b) Semiquantitative determination of trans-vacant and cis-vacant 2:1 layers in illites and illite-smectites by thermal analysis and X-ray diffraction. *American Mineralogist*, **83**, 1188–1198.

Durand, B. (1985) Diagenetic modifications of kerogens. *Philosophical Transactions of the Royal Society of London*, **315A**, 77–90.

Dypvik, H. (1983) Clay mineral transformations in Tertiary and Mesozoic sediments from North Sea. *American Association of Petroleum Geologists Bulletin*, **67**, 160–165.

Eberl, D. (1986) Sodium-potassium ion exchange during smectite diagenesis – A theoretical discussion. Pp. 363–368 in: *Studies in Diagenesis* (F.A. Mumpton, editor). *US Geological Survey Bulletin*, **1578**.

Foscolos, A.E. and Powell, T.G. (1979) Mineralogical and geochemical transformation of clays during burial diagenesis (catagenesis): relation to oil generation. Pp. 261–270 in: *Proceedings of the International Clay Conference, Oxford* (M.M. Mortland and V.C. Farmer, editors). Developments in Sedimentology, **27**. Elsevier, Amsterdam.

Gaultier, J. and Mamy, J. (1979) Etude comparee de l'evolution des montmorillonites biioniques K-Ca de Camp Berteaux et du Wyoming sous l'effet des cycles d'humifica-

tion et de dessication. *Clay Minerals*, **14**, 181–192.

Gaultier, J. and Mamy, J. (1982) Demixing phenomenon in low water content biionic K-Na montmorillonites. Pp. 451–457 in: *Proceedings of the International Clay Conference, Bologna and Pavia* (H. van Olphen and F. Veniale, editors). Elsevier, Amsterdam.

Hansen, P.L. and Lindgreen, H. (1989) Mixed-layer illite/smectite diagenesis in Upper Jurassic claystones from the North Sea and onshore Denmark. *Clay Minerals,* **24**, 197–213.

Heling, D. and Teichmuller, K. (1974) Die Grenze Montmorillonit/Mixed Layer-Minerale und ihre Beziehung zur Inkohlung in der grauen Schichtenfolge des Oligozäns im Oberrheingraben. *Fortschritte der Geologie von Rheinland und Westfalen*, **24**, 113–128.

Higashi, S. (1978) Dioctahedral mica minerals with ammonium ions. *Mineralogical Journal*, **9**, 16–27.

Hood, A., Gutjahr, C.C.M. and Heacock, R.L. (1975) Organic metamorphism and the generation of petroleum. *American Association of Petroleum Geologists Bulletin*, **59**, 986–996.

Hower, J., Eslinger, E.V., Hower, M.E. and Perry, E.A. (1976) Mechanism of burial metamorphism of argillaceous sediments. *Geological Society of America Bulletin,* **87**, 725–737.

Hunt, J.M. (1979) *Petroleum Geochemistry and Geology.* W.H. Freeman & Co., San Francisco.

Jakobsen, H.J., Daugaard, P. and Langer, V. (1988) CP/MAS NMR at high speeds and high fields. *Journal of Magnetic Resonance*, **76**, 162–168.

Jensenius, J. (1987) High-temperature diagenesis in shallow chalk reservoir, Skjold oil field, Danish North Sea: Evidence from fluid inclusions and oxygen isotopes. *American Association of Petroleum Geologists Bulletin*, **71**, 1378–1386.

Johnston, J.H. and Cardile, C.M. (1987) Iron substitution in montmorillonite, illite and glauconite by ^{57}Fe Mössbauer spectroscopy. *Clays and Clay Minerals*, **35**, 170–176.

Juster, T.C., Brown, P.E. and Bailey, S.W. (1987) NH_4-bearing illite in very low grade metamorphic rocks associated with coal, northeastern Pennsylvania. *American Mineralogist*, **72**, 555–565.

Karyakin, A.V., Volynets, V.F. and Kriventsova, G.A. (1973) Investigation of nitrogen compounds in micas by infrared spectroscopy. *Geokhimiya*, **3**, 439–442.

Lindgreen, H. (1991) Elemental and structural changes in illite/smectite mixed-layer clay minerals during diagenesis in Kimmeridgian-Volgian(-Ryazanian) clays in the Central Trough. *Bulletin of the Geological Society of Denmark*, **39**, 1–82.

Lindgreen, H. (1994) Ammonium fixation during illite-smectite diagenesis in Upper Jurassic shale, North Sea. *Clay Minerals*, **29**, 527–537.

Lindgreen, H. and Hansen, P.L. (1991) Ordering of illite-smectite in Upper Jurassic claystones from the North Sea. *Clay Minerals*, **26**, 105–125.

Lindgreen, H., Jacobsen, H. and Jakobsen, H.J. (1991) Diagenetic structural transformations in North Sea Jurassic illite/smectite. *Clays and Clay Minerals*, **39**, 54–69.

Lindgreen, H., Garnaes, J., Besenbacher, F., Laegsgaard, E. and Stensgaard, I. (1992) Illite-smectite from the North Sea investigated by scanning tunnelling microscopy. *Clay Minerals,* **27**, 331–342.

Lindgreen, H., Drits, V.A., Sakharov, B.A., Salyn, A., Wrang, P. and Dainyak, L. (2000) Illite-smectite structural changes during metamorphism in black Cambrian Alum shales from the Baltic area. *American Mineralogist*, **85**, 1223–1238.

Meunier, A. and Velde, B. (1989) Solid solutions in I/S mixed-layer minerals and illite. *American Mineralogist*, **74**, 1106–1112.

Moore, D.M. and Reynolds, R.C. (1989) *X-ray diffraction and the Identification and Analysis of Clay Minerals.* Oxford University Press, Oxford, UK.

Morgan, D.J. (1977) Simultaneous DTA-EGA of minerals and natural mineral admixtures. *Journal of Thermal Analysis*, **12**, 245–263.

Nadeau, P.H. and Bain, D.C. (1986) Composition of some smectites and diagenetic illitic clays and implications for their origin. *Clays and Clay Minerals*, **34**, 455–464.

Nadeau, P.H., Wilson, M.J., McHardy, W.J. and Tait, J.M. (1985) The conversion of smectite to illite during diagenesis: evidence from some illitic clays from bentonites and sandstones. *Mineralogical Magazine*, **49**, 393–400.

Perry, E. and Hower, J. (1970) Burial diagenesis in Gulf Coast pelitic sediments. *Clays and Clay Minerals,* **18**, 165–177.

Pollard, C.O. (1971) Semi-displacive mechanism for diagenetic alteration of montmorillonite layers to illite layers. *Geological Society of America, Special Paper*, **134**, 79–96.

Sakharov, B.A., Lindgreen, H., Salyn, A.L. and Drits, V.A. (1999) Determination of illite-smectite structures using multispecimen XRD profile fitting. *Clays and Clay Minerals*, **47**, 555–566.

Shutov, V.D., Drits, V.A. and Sakharov, B.A. (1969a) On the mechanism of a postsedimentary transformation of montmorillonite into hydromica. Pp. 523–532 in: *Proceedings of the International Clay Conference, Tokyo,* Vol. **1** (L. Heller, editor). Jerusalem.

Shutov, V.D., Drits, V.A. and Sakharov, B.A. (1969b) On the mechanism of a postsedimentary transformation of montmorillonite into hydromica: discussion. Pp. 126–129 in: *Proceedings of the International Clay Conference, Tokyo,* Vol. **2** (L. Heller, editor). Jerusalem.

Środoń, J., Elsass, F., McHardy, W.J. and Morgan, D.J. (1992) Chemistry of illite-smectite inferred from TEM measurements of fundamental particles. *Clays Minerals*, **27**, 137–158.

Środoń, J., Eberl, D.D. and Drits, V.A. (2000) Evolution of fundamental-particle size during illitization of smectite and implications for reaction mechanism. *Clays and Clay Minerals*, **48**, 446–458.

Stevenson, F.J. (1960) Nitrogeneous constituents of some palaeozoic shales (abs.) *American Association of Petroleum Geologists Bulletin*, **44**, 1257.

Thomsen, E., Lindgreen, H. and Wrang, P. (1983) Investigation on the source rock potential of Denmark. *Geologie en Mijnbouw*, **62**, 221–239.

Tissot, B. and Welte, D.H. (1978) *Petroleum Formation and Occurrence. A new Approach to Oil and Gas Exploration.* Springer Verlag, Berlin.

Tsipursky, S.I. and Drits, V.A. (1984) The distribution of octahedral cations in the 2:1 layers of dioctahedral smectites studied by oblique-texture electron diffraction. *Clay Minerals*, **19**, 177–193.

Vedder, W. (1965) Ammonium in muscovite. *Geochimica et Cosmochimica Acta*, **29**, 221–228.

Williams, L.B., Ferrell, R.E., Jr., Chinn, E.W. and Sassen, R. (1989) Fixed-ammonium in clays associated with crude oils. *Applied Geochemistry*, **4**, 605–616.

Williams, L.B., Wilcoxon, B.R., Ferrell, R.E. and Sassen, R. (1992) Diagenesis of ammonium during hydrocarbon maturation and migration, Wilcox Group, Louisiana, USA. *Applied Geochemistry*, **7**, 123–134.

Yamamoto, T. and Nakahira, M. (1966) Ammonium ions in sericites. *American Mineralogist*, **51**, 1775–1778.

(*Received 24 January 2001; revised 5 June 2001; Ms. 517*)